ISME

Robust Sliding Mode Control of Nonlinear Ship Autopilot System

F. Rashidi[*]
Assistant Professor

A. Harifi[†]
Assistant Professor

Designing of ship autopilot is a challenging problem because of high nonlinearity of ship dynamics and various acting disturbances. The goal of this research work is to design a robust and efficient sliding mode control for ship autopilot system. The main contribution is to employ a nonlinear dynamic model bound of uncertainties for controller design. In order to reduce the side effects of chattering phenomenon, integral switching variable is used to modify the proposed control technique. Simulation results in the rough wave condition show that the proposed sliding mode control method is able to cope with nonlinearity, uncertainty, and disturbances in the system. Moreover, the controller significantly reduces the chattering in comparison with a previous similar research.

DOI: 10.30506/jmee.2020.118967.1220

Keywords: Sliding Mode Control, Integral Switching Variable, Nonlinear Controller, Ship Autopilot.

1 Introduction

Robust control of ship autopilot system is one of the most challenging topics in the field of automatic control theory [1]. This is due to the fact that the dynamic model of the system *is* nonlinear and uncertain. In the last few years, many various control methods are proposed to control the ship autopilot system such as optimal control [2], intelligent control [3], neural network control [4], adaptive control [5], sliding mode control (SMC) [6], fuzzy control [7], fuzzy sliding mode control [8], backstepping control [9, 10], neural control based Kalman filter [11], genetic algorithm based control [12] and robust control [13]. However, because of body-fixed rotation frame associated with the inertial frame and also existence of nonlinear damping terms, the dynamic model of autopilot ship is nonlinear [6]. Although, linearization of the nonlinear model and design of a control system based on the linear model is common, however, the designed controller cannot guarantee the stability of the system under study [14]. On the other hand, there are many parameter uncertainties in the ship dynamic system which are due to waves, trim, environmental disturbance and loading [10].

[*]Corresponding Author, Assistant Professor, Faculty of Engineering, University of Hormozgan, Bandar-Abbas, Iran rashidi@hormozgan.ac.ir

[†]Assistant Professor, Faculty of Engineering, University of Hormozgan, Bandar-Abbas, Iran harifi@hormozgan.ac.ir

Receive : 2019/12/22 Accepted : 2020/07/24

Therefore, to overcome these limitations and drawbacks and also to find optimal solution scheme for control of ship autopilot system, several nonlinear and robust control techniques are introduced in the literature [15]. Sliding mode control technique is one of the most important and common control algorithms which is designed to control the nonlinear system with uncertainty. Although many research studies are introduced in the designing of sliding mode control method for ship autopilot system, however, a surveys show most of them have the same structure which is based on Fossen previous work [16]. In another research, three SMCs based on different transfer functions (Rudder-Yaw, Rudder-Roll and Fin-Roll) are compared with PID controller [17]. Also in [18], a sliding mode control method is designed for ship autopilot and the total system is simulated based on nonlinear hydrodynamic model. However, it should be noted that in these studies the linearized model of ship are used for design of the control method, moreover, the uncertainty bound is not calculated analytically.
In this study, at the first step, a SMC technique is designed for the nonlinear dynamic model of the ship with parameter uncertainty. Then the proposed control approach is modified using integral switching variable (ISV). Results show that the method presented in this paper has better performance than the similar case.

The paper is organized as the following. Section 2 presents a nonlinear dynamic model of ship with parameter uncertainty. The mathematical equations of hydrodynamic and rudder forces-moments are described in section 3 and 4 respectively. The controller designing procedure is described in section 5. After that, the related uncertainties bounds are calculated in section 6. The modified SMC based on ISV is presented in section 7. In section 8, the performance of the controller is verified and compared. Finally the conclusion and future challenges are presented in section 9.

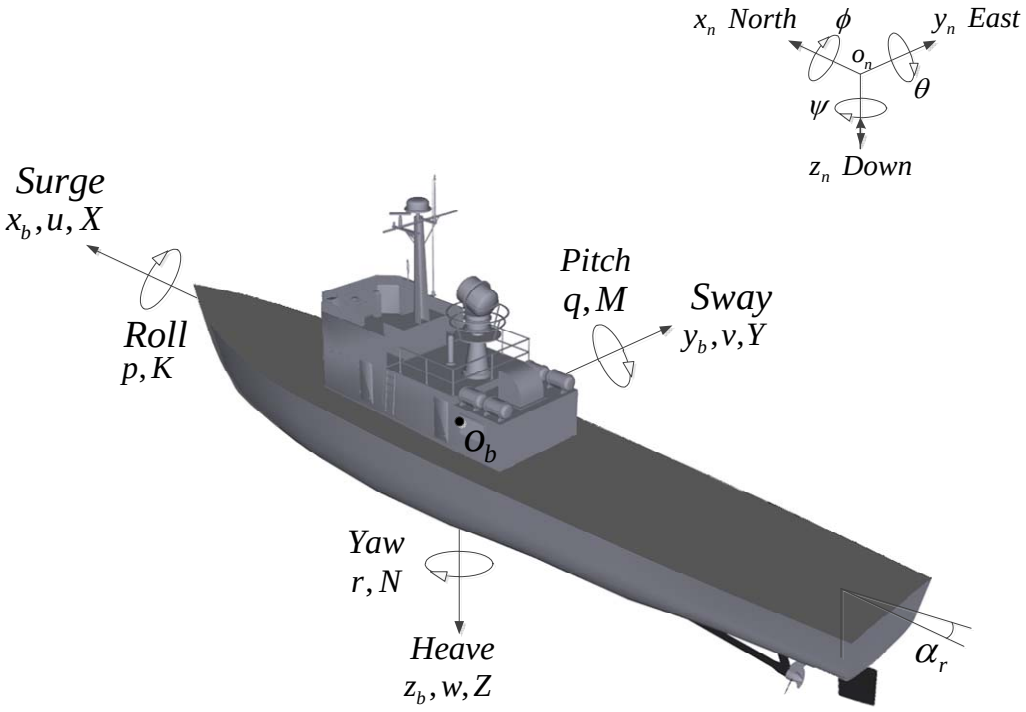

Figure 1 Sign conventions and Standard notation of ship motion [19]

2 Ship dynamic

Ship motion in sailing condition has 6 degrees of freedom which include 3 translational DOF entitled Surge, Sway and Heave and 3 rotational DOF entitled Roll, Pitch and Yaw. As shown in Figure (1), the orientation $[\phi,\theta,\psi]^T$ and position $[x_n, y_n, z_n]^T$ of a ship are usually described in an inertial frame and forces $[X,Y,Z]^T$, linear velocities $[u,v,w]^T$,moments $[K,M,N]^T$, and angular velocities $[p,q,r]^T$ are described in a body-fixed frame.
Define position-orientation vector $\boldsymbol{\eta}$ and linear-angular velocity $\boldsymbol{\upsilon}$ as follow [19]:

$$\boldsymbol{\eta} \triangleq [x_n, y_n, z_n, \phi, \theta, \psi]^T \tag{1}$$

$$\boldsymbol{\upsilon} \triangleq [u, v, w, p, q, r]^T \tag{2}$$

Then the translation matrix $\mathbf{J}_b^n(\phi,\theta,\psi)$ can be found so that:

$$\dot{\boldsymbol{\eta}} = \mathbf{J}_b^n(\phi,\theta,\psi)\boldsymbol{\upsilon} \tag{3}$$

Using Newtonian method, motion equations in body-fixed reference frame can be expressed as follow:

$$\mathbf{M}_{RB}^b\dot{\boldsymbol{\upsilon}} + \mathbf{C}_{RB}^b(\boldsymbol{\upsilon})\boldsymbol{\upsilon} = \boldsymbol{\tau}^b \tag{4}$$

Where $\boldsymbol{\tau}^b \triangleq [X,Y,Z,K,M,N]^T$, $\mathbf{M}_{RB}^b$ is mass and inertia matrix and the term $\mathbf{C}_{RB}^b(\boldsymbol{\upsilon})\boldsymbol{\upsilon}$ arise from the coriolis and centripetal forces and moments. Each element of the forces-moments vector, $\boldsymbol{\tau}^b$, could be originated from different phenomena.

$$\boldsymbol{\tau}^b = \boldsymbol{\tau}_{hyd} + \boldsymbol{\tau}_{cs} + \boldsymbol{\tau}_{prop} + \boldsymbol{\tau}_{ext} \tag{5}$$

The elements are defined as follow:

$\boldsymbol{\tau}_{hyd}$: Represents hydrodynamic forces-moments (hull movement in the sea).

$\boldsymbol{\tau}_{cs}$: is produced by control surfaces such as rudder and fins.

$\boldsymbol{\tau}_{prop}$: The propulsion systems such as propellers and thrusters generate this part.

$\boldsymbol{\tau}_{ext}$: is due to environmental disturbances.

Usually, Pitch and Heave motions can be neglected. We suppose that the forward speed of the ship is constant. Hence, using equation (4), 3 DOF (Sway, Roll and Yaw) equations of ship motion can be illustrated in the state space form as follow [20]:

$$\begin{bmatrix} \dot{v} \\ \dot{p} \\ \dot{r} \end{bmatrix} = \mathbf{M}^{-1}\left(\begin{bmatrix} -mur \\ mz_g^b ur \\ -mx_g^b ur \end{bmatrix} + \begin{bmatrix} Y_{hyd}^* \\ K_{hyd}^* \\ N_{hyd}^* \end{bmatrix} + \begin{bmatrix} Y_{cs} \\ K_{cs} \\ N_{cs} \end{bmatrix}\right) \tag{6}$$

Where ,

$$\mathbf{M} = \begin{bmatrix} \left(m - Y_{\dot{v}}\right) & -\left(mz_g^b + Y_{\dot{p}}\right) & \left(mx_g^b - Y_{\dot{r}}\right) \\ -\left(mz_g^b + K_{\dot{v}}\right) & \left(I_{xx}^b - K_{\dot{p}}\right) & -K_{\dot{r}} \\ \left(mx_g^b - N_{\dot{v}}\right) & -N_{\dot{p}} & \left(I_{zz}^b - N_{\dot{r}}\right) \end{bmatrix} \tag{7}$$

which m is total mass of the ship, I_{xx}^b and I_{zz}^b are the inertias about x_b and z_b axes, x_g^b and z_g^b are the positions of gravity center in x and z axes of body-fixed frame, and $Y_{\dot{v}}$, $Y_{\dot{p}}$, $Y_{\dot{r}}$, $K_{\dot{v}}$, $K_{\dot{p}}$, $K_{\dot{r}}$, $N_{\dot{v}}$, $N_{\dot{p}}$ and $N_{\dot{r}}$ are hydrodynamic derivatives. (Refer to section 3)
Using equation (3), we have:

$$\begin{aligned} \dot{\phi} &= p \\ \dot{\psi} &= r\cos\phi \end{aligned} \tag{8}$$

According to equation (8), there is a nonlinear relationship between $\dot{\psi}$ and ϕ, however, in the most of ships, ϕ is less than 3 degrees and hence, this relationship can be considered as the linear function(i.e., $\cos\phi = 1$). Therefore, in the above equation we have $\dot{\psi} = r$ [21].

3 Hydrodynamic forces-moments

The hydrodynamic forces-moment is a complex phenomenon which is hard to model by traditional methodologies. However, this phenomenon can be considered by some nonlinear functions and variables such as accelerations, velocities, and Euler angles. Hence, at stated in [20], it is usual to express this by the series expansion which its coefficients are obtained based on some experiments on small-scale ship. For the desired ship, this can be represent at the fowling [20]:

$$\begin{aligned} Y_{hyd} &= Y_{\dot{v}}\dot{v} + Y_{\dot{r}}\dot{r} + Y_{\dot{p}}\dot{p} \\ &\quad + Y_{|u|v}|u|v + Y_{ur}ur + Y_{v|v|}v|v| + Y_{v|r|}v|r| + Y_{r|v|}r|v| \\ &\quad + Y_{\phi|uv|}\phi|uv| + Y_{\phi|ur|}\phi|ur| + Y_{\phi uu}\phi u^2 \\ K_{hyd} &= K_{\dot{v}}\dot{v} + K_{\dot{r}}\dot{r} + K_{\dot{p}}\dot{p} \\ &\quad + K_{|u|v}|u|v + K_{ur}ur + K_{v|v|}v|v| + K_{v|r|}v|r| + K_{r|v|}r|v| \\ &\quad + K_{\phi|uv|}\phi|uv| + K_{\phi|ur|}\phi|ur| + K_{\phi uu}\phi u^2 + K_{|u|p}|u|p \\ &\quad + K_{p|p|}p|p| + K_p p + K_{\phi\phi\phi}\phi^3 - \rho g\nabla GMt \\ N_{hyd} &= N_{\dot{v}}\dot{v} + N_{\dot{r}}\dot{r} + N_{\dot{p}}\dot{p} \\ &\quad + N_{|u|v}|u|v + N_{|u|r}|u|r + N_{r|r|}r|r| + N_{r|v|}r|v| \\ &\quad + N_{\phi|uv|}\phi|uv| + N_{\phi u|r|}\phi|ur| + N_{\phi u|u|}\phi u|u| \end{aligned} \tag{9}$$

Where $Y_{\dot{v}}$, $Y_{\dot{r}}$, $Y_{\dot{p}}$, $Y_{|u|v}$, Y_{ur}, $Y_{v|v|}$, $Y_{v|r|}$, $Y_{r|v|}$, $Y_{\phi|uv|}$, $Y_{\phi|ur|}$, $Y_{\phi uu}$, $K_{\dot{v}}$, $K_{\dot{r}}$, $K_{\dot{p}}$, $K_{|u|v}$, K_{ur}, $K_{v|v|}$, $K_{v|r|}$, $K_{r|v|}$, $K_{\phi|uv|}$, $K_{\phi|ur|}$, $K_{\phi uu}$, $K_{|u|p}$, $K_{p|p|}$, K_{p}, $K_{\phi\phi\phi}$, $N_{\dot{v}}$, $N_{\dot{r}}$, $N_{\dot{p}}$, $N_{|u|v}$, $N_{|u|r}$, $N_{r|r|}$, $N_{r|v|}$, $N_{\phi|uv|}$, $N_{\phi u|r|}$ and $N_{\phi u|u|}$ are constant coefficients called hydrodynamic derivatives.

Also g is gravity constant, ρ is water density, ∇ is displacement volume and GMt is transverse metacentric height. Note that Y^*_{hyd}, K^*_{hyd} and N^*_{hyd} are obtained by eliminating the first rows of equation (9).

4 Rudder forces-moments

The rudder forces-moments can be calculated as the following equations [1]:

$$\begin{aligned} Y_{cs} &\approx L \\ K_{cs} &\approx -r_r.L \\ N_{cs} &\approx -LCG.L \end{aligned} \tag{10}$$

Where r_r is vertical distance between gravity center and pressure center, LCG is the horizontal distance between gravity center and the rudder's rotational axis. Parameter L is obtained by using the following formula:

$$L \approx \frac{1}{2}\rho u_r^2 A_r \left.\frac{\partial C_L}{\partial \alpha_r}\right|_{\alpha_r=0} \alpha_r \tag{11}$$

In this equation, A_r is the area of the rudder, α_r is rudder angle, u_r is the water speed average. The parameter $\left.\frac{\partial C_L}{\partial \alpha_r}\right|_{\alpha_r=0}$ is also a constant coefficient.

It is worth mention that the rudder is the behind of ship propeller. Hence, the ship speed and the flow passed through the rudder are not equal. The flow can be calculated by the following equation [10]:

$$u_p = \frac{1}{2}\left[(1-w)u + \sqrt{(1-w)^2 u^2 + \frac{2(1-t)^{-1} X_{u|u|} u|u|}{\rho A_p}}\right] \tag{12}$$

where u is ship speed, w is wake fraction, t is thrust deduction number, A_p is propeller area, and $X_{u|u|}$ is a hydrodynamic constant of water resistance. The radius of the wake at a location of x meters behind the propeller can be estimated as [10]:

$$r(x) = r_p \frac{0.14\left(\frac{u_p}{2u_p - u_a}\right) + \left(\frac{x}{r_p}\right)^{1.5}}{0.14\left(\frac{u_p}{2u_p - u_a}\right)^{1.5} + \left(\frac{x}{r_p}\right)^{1.5}} \sqrt{\frac{u_p}{2u_p - u_a}} \tag{13}$$

Where r_p is radius of propeller and $u_a = (1-w)u$. Finally, passing flow through the rudder can be calculated as:

$$u_r = u_p \left(\frac{r_p}{r(x)} \right)^2 \tag{14}$$

5 Sliding mode controller design

The important mission of an autopilot system is determination of rudder angle, such that the heading of ship tracks a desired value. In this study, to achieve the goal, a robust sliding mode controller is proposed for the control of ship autopilot system with parameter uncertainties. It is supposed that the effect of rudder angle in Roll angle is negligible so the Roll angle can be considered zero. To control Yaw angle, a switching variable can be defined as follow:

$$\sigma = \dot{\tilde{\psi}} + c\tilde{\psi} \tag{15}$$

Where $\tilde{\psi} = \psi - \psi_d$, ψ_d is desired value of heading and c is a constant value. Therefore, if σ is controlled at zero then ψ will be reached to ψ_d. Equation (6) can be rewritten as:

$$\begin{aligned} \dot{\psi} &= r \\ \dot{r} &= f + g\delta \end{aligned} \tag{16}$$

Where

$$\begin{aligned} f &= w_{31}\left(Y^*_{hyd} - mur\right) + w_{32}\left(K^*_{hyd} + z^b_g mur\right) + w_{33}\left(N^*_{hyd} - x^b_g mur\right) \\ g &= \frac{1}{2}\left(-w_{31} + r_r \cdot w_{32} + LCG \cdot w_{33}\right)\rho u_r^2 A_r \left.\frac{\partial C_{Lr}}{\partial \alpha_r}\right|_{\alpha_r = 0} \\ \delta &= -\alpha_r \end{aligned} \tag{17}$$

In the equation (17), $w_{ij}\left(1 \le i, j \le 3\right)$ is $\left(i, j\right)^{\text{th}}$ element of $\mathbf{W}$ where $\mathbf{W} = \mathbf{M}^{-1}$. It is necessary to note that for designing a sliding mode controller, the function g should be greater than zero in (16). So, for satisfying this condition the virtual control input is defined as $\delta = -\alpha_r$.

The control problem for designing an autopilot is defined as the following:

It is necessary to find out the main control input α_r so that in the presence of uncertainties (i.e., $\left| f - \hat{f} \right| \le F$ and $g_{\min} \le g \le g_{\max}$), the variables ψ and its derivative r ,which stated in (16), can track the prescribed desired values ψ_d and $\dot{\psi}_d$ respectively.

The main objective of sliding mode control system is to design the control input such that switching variable reaches zero in finite time and remain at this value [22]. For this purpose, a Lyapunov function is considered as follows:

$$V = \frac{1}{2}\sigma^2 \tag{18}$$

Differentiating from equation (18) and using equations (15) and (16):

$$\begin{aligned}\dot{V} &= \sigma\dot{\sigma} \\ &= \sigma\left(\ddot{\psi} - \ddot{\psi}_d + c\left(\dot{\psi} - \dot{\psi}_d\right)\right) \\ &= \sigma\left(f - \ddot{\psi}_d + c\left(r - \dot{\psi}_d\right) + g\delta\right)\end{aligned} \tag{19}$$

Obviously, $\dot{V}$ must be smaller than zero to guaranty that switching variable will be reached to zero. But it is necessary to note that the precise value of f and g are not known. So, we consider the control input as follow:

$$\delta = \delta_{eq} + \delta_{sw} \tag{20}$$

Where

$$\begin{aligned}\delta_{eq} &= \frac{-\hat{f} + \ddot{\psi}_d + c\left(\dot{\psi}_d - r\right)}{\hat{g}} \\ \delta_{sw} &= \frac{-k \cdot sign(\sigma)}{\hat{g}}\end{aligned} \tag{21}$$

In the above equations, the variables with hat sign are nominal values of the variables. The variable δ_{eq} is equivalent control that tries to eliminate nonlinear and known terms of equation. δ_{sw} is switching control that compensates the system uncertainties, The parameter k is the switching control signal gain that should be determined. By substituting equations (20) and (21) into (19):

$$\begin{aligned}\dot{V} &= \sigma\left(f - \hat{f}\frac{g}{\hat{g}} + \left(-\ddot{\psi}_d + c\left(r - \dot{\psi}_d\right)\right)\left(1 - \frac{g}{\hat{g}}\right) - k \cdot sign(\sigma)\frac{g}{\hat{g}}\right) \\ &= \sigma\left(f - \hat{f} + \left(\hat{f} - \ddot{\psi}_d + c\left(r - \dot{\psi}_d\right)\right)\left(1 - \frac{g}{\hat{g}}\right) - k \cdot sign(\sigma)\frac{g}{\hat{g}}\right) \\ &\le |\sigma|\left|f - \hat{f}\right| + |\sigma|\left|\hat{g}\delta_{eq}\right|\left|1 - \frac{g}{\hat{g}}\right| - k|\sigma|\frac{g}{\hat{g}} \le 0\end{aligned} \tag{22}$$

So, k must satisfy the following inequality:

$$k \ge \frac{\hat{g}}{g}\left|f - \hat{f}\right| + \left|\hat{g}\delta_{eq}\right|\left|\frac{\hat{g}}{g} - 1\right| \tag{23}$$

Now, we suppose that the bounds of uncertainties are known as follow:

$$\begin{aligned}&\left|f - \hat{f}\right| \le F \\ &0 < g_{\min} \le g \le g_{\max} \quad , \quad \hat{g} = \sqrt{g_{\min} g_{\max}}\end{aligned} \tag{24}$$

So, for satisfying equation (23) a simple choice is:

$$k = \gamma F + (\gamma - 1)\left|\hat{g}\delta_{eq}\right| + \varepsilon \tag{25}$$

Where ε is a positive constant and

$$\gamma = \sqrt{\frac{g_{\max}}{g_{\min}}} \tag{26}$$

Finally we have:

$$\alpha_r = \frac{\hat{f} - \ddot{\psi}_d + c\left(r - \dot{\psi}_d\right) + \left(\gamma F + (\gamma - 1)\left|\hat{f} - \ddot{\psi}_d + c\left(r - \dot{\psi}_d\right)\right| + \varepsilon\right) sign(\sigma)}{\hat{g}} \tag{27}$$

6 Uncertainty Bounds

One of the main tasks in sliding mode controller design is to determine the proper values of uncertainty bounds. If the uncertainty bounds are chosen less than actual values, the control system cannot provide the stability and might get unstable. On the other hand, choice of bounds in a conservative way can lead to an unacceptable phenomenon, such as chattering, which results in significant control signal energy. To consider uncertainty bounds, we assume that four parameters inertia, ship mass, gravity center and hydrodynamic coefficients are varied about $\pm n\%$ around their nominal values. For example, the mass of ship m, can varied in the range of $\left(1-\frac{n}{100}\right)\hat{m} \le m \le \left(1+\frac{n}{100}\right)\hat{m}$.

Analytical calculation of lower and upper bounds of elements in matrix $\mathbf{M}^{-1}$ are very costly. Hence, in this study, Genetic Algorithm (GA) is used to determine the variation ranges of the elements. To do this, an individual with 14 genes $[x_1, x_2, ..., x_{14}]$ is considered. Each gene can take values between $\left(1-\frac{n}{100}\right)$ and $\left(1+\frac{n}{100}\right)$. Then by following equation (28) and substituting them into (7), the invers of matrix $\mathbf{M}$ is calculated and in the last step, GA determines the minimum (w_{ij}^{-}) and maximum (w_{ij}^{+}) values of each element (w_{ij} $1 \le i, j \le 3$).

$$\begin{aligned}
&m = \hat{m}.x_1 && I_{xx}^b = \hat{I}_{xx}^b.x_2 && I_{zz}^b = \hat{I}_{zz}^b.x_3 \\
&x_g^b = \hat{x}_g^b.x_4 && z_g^b = \hat{z}_g^b.x_5 && Y_{\dot{v}} = \hat{Y}_{\dot{v}}.x_6 \\
&Y_{\dot{p}} = \hat{Y}_{\dot{p}}.x_7 && Y_{\dot{r}} = Y_{\dot{r}}.x_8 && K_{\dot{v}} = \hat{K}_{\dot{v}}.x_9 \\
&K_{\dot{p}} = \hat{K}_{\dot{p}}.x_{10} && K_{\dot{r}} = \hat{K}_{\dot{r}}.x_{11} && N_{\dot{v}} = \hat{N}_{\dot{v}}.x_{12} \\
&N_{\dot{p}} = \hat{N}_{\dot{p}}.x_{13} && N_{\dot{r}} = \hat{N}_{\dot{r}}.x_{14}
\end{aligned} \tag{28}$$

With these assumptions, the following equation can be written:

$$\begin{aligned}
\left|f - \hat{f}\right| \le{}& \left|w_{31}Y_{hyd}^* - \hat{w}_{31}\hat{Y}_{hyd}^*\right| + \left|w_{32}K_{hyd}^* - \hat{w}_{32}\hat{K}_{hyd}^*\right| + \left|w_{33}N_{hyd}^* - \hat{w}_{33}\hat{N}_{hyd}^*\right| \\
&+ \left|w_{31}mur - \hat{w}_{31}\hat{m}ur\right| + \left|w_{32}z_g^b mur - \hat{w}_{32}\hat{z}_g^b\hat{m}ur\right| + \left|w_{33}x_g^b mur - \hat{w}_{33}\hat{x}_g^b\hat{m}ur\right|
\end{aligned} \tag{29}$$

Using the triangle inequality $\left|a_1 + a_2 + \cdots + a_n\right| \le \left|a_1\right| + \left|a_2\right| + \cdots + \left|a_n\right|$, each term of equation (29) can be expanded. For example,

$$\begin{aligned}
\left|w_{31}Y_{hyd}^* - \hat{w}_{31}\hat{Y}_{hyd}^*\right| &\le \left|w_{31}Y_{|u|v}|u|v - \hat{w}_{31}\hat{Y}_{|u|v}|u|v\right| + \left|w_{31}Y_{ur}ur - \hat{w}_{31}\hat{Y}_{ur}ur\right| + \cdots \\
&\le \left|w_{31}Y_{|u|v} - \hat{w}_{31}\hat{Y}_{|u|v}\right|\left|uv\right| + \left|w_{31}Y_{ur} - \hat{w}_{31}\hat{Y}_{ur}\right|\left|ur\right| + \cdots
\end{aligned} \tag{30}$$

Equation (30) shows that it is required to find the maximum value of equations in form of $\left|w_{\circ}Y_{\square}-\hat{w}_{\circ}\hat{Y}_{\square}\right|$. Assuming that the difference between real and nominal values of $w_{\circ}$ and $Y_{\square}$ variables are $\Delta w_{\circ}$ and $\Delta Y_{\square}$ respectively, we have:

$$\begin{aligned}\left|w_{\circ}Y_{\square}-\hat{w}_{\circ}\hat{Y}_{\square}\right| &= \left|\left(\hat{w}_{\circ}+\Delta w_{\circ}\right)\left(\hat{Y}_{\square}+\Delta Y_{\square}\right)-\hat{w}_{\circ}\hat{Y}_{\square}\right| \\ &= \left|\hat{w}_{\circ}\Delta Y_{\square}+\Delta w_{\circ}\hat{Y}_{\square}+\Delta w_{\circ}\Delta Y_{\square}\right| \\ &\le \left|\hat{w}_{\circ}\Delta Y_{\square}\right|+\left|\Delta w_{\circ}\hat{Y}_{\square}\right|+\left|\Delta w_{\circ}\Delta Y_{\square}\right|\end{aligned} \tag{31}$$

Assuming $\hat{\mathbf{W}}=\frac{1}{2}\left(\mathbf{W}^{+}+\mathbf{W}^{-}\right)$, it can be obtained that $\left|\Delta w_{\circ}\right|\le\frac{1}{2}\left(w_{\circ}^{+}-w_{\circ}^{-}\right)$. Furthermore, based on the assumption that there is n% uncertainty in hydrodynamic coefficients, we have $\left|\Delta Y_{\square}\right|\le\frac{n}{100}\left|Y_{\square}\right|$. So, the equation (31) can be expanded as follow:

$$\begin{aligned}\left|w_{\circ}Y_{\square}-\hat{w}_{\circ}\hat{Y}_{\square}\right| &\le \left|\hat{w}_{\circ}\Delta Y_{\square}\right|+\left|\Delta w_{\circ}\hat{Y}_{\square}\right|+\left|\Delta w_{\circ}\Delta Y_{\square}\right| \\ &\le \left|\hat{w}_{\circ}\right|\frac{n}{100}\left|\hat{Y}_{\square}\right|+\frac{w_{\circ}^{+}-w_{\circ}^{-}}{2}\left|\hat{Y}_{\square}\right|+\frac{w_{\circ}^{+}-w_{\circ}^{-}}{2}\frac{n}{100}\left|\hat{Y}_{\square}\right| \\ &= \left(\left|\frac{w_{\circ}^{+}+w_{\circ}^{-}}{2}\right|\frac{n}{100}+\frac{w_{\circ}^{+}-w_{\circ}^{-}}{2}\left(1+\frac{n}{100}\right)\right)\left|\hat{Y}_{\square}\right|\end{aligned} \tag{32}$$

Finally, using equation (32) we have:

$$\begin{aligned}F=&\left[\frac{n}{100}\left|\frac{w_{31}^{+}+w_{31}^{-}}{2}\right|+\left(1+\frac{n}{100}\right)\left(\frac{w_{31}^{+}-w_{31}^{-}}{2}\right)\right]\left(\begin{array}{l}\left|\hat{Y}_{|u|v}uv\right|+\left|\hat{Y}_{ur}ur\right|+\left|\hat{Y}_{v|v|}v^{2}\right|+\left|\hat{Y}_{v|r|}vr\right|+\left|\hat{Y}_{r|v|}rv\right| \\ +\left|\hat{Y}_{\phi|uv|}\phi uv\right|+\left|\hat{Y}_{\phi|ur|}\phi ur\right|+\left|\hat{Y}_{\phi uu}\phi u^{2}\right|+\left|\hat{m}ur\right|\end{array}\right) \\ &+\left[\frac{n}{100}\left|\frac{w_{32}^{+}+w_{32}^{-}}{2}\right|+\left(1+\frac{n}{100}\right)\left(\frac{w_{32}^{+}-w_{32}^{-}}{2}\right)\right]\times\left(\begin{array}{l}\left|\hat{K}_{|u|v}uv\right|+\left|\hat{K}_{ur}ur\right|+\left|\hat{K}_{v|v|}v^{2}\right|+\left|\hat{K}_{v|r|}vr\right|+\left|\hat{K}_{r|v|}rv\right| \\ +\left|\hat{K}_{\phi|uv|}\phi uv\right|+\left|\hat{K}_{\phi|ur|}\phi ur\right|+\left|\hat{K}_{\phi uu}\phi u^{2}\right| \\ +\left|\hat{K}_{|u|p}up\right|+\left|\hat{K}_{p|p|}p^{2}\right|+\left|\hat{K}_{p}p\right|+\left|\hat{K}_{\phi\phi\phi}\phi^{3}\right|\end{array}\right) \\ &+\left[\frac{n}{100}\left|\frac{w_{33}^{+}+w_{33}^{-}}{2}\right|+\left(1+\frac{n}{100}\right)\left(\frac{w_{33}^{+}-w_{33}^{-}}{2}\right)\right]\times\left(\begin{array}{l}\left|\hat{N}_{|u|v}uv\right|+\left|\hat{N}_{|u|r}ur\right|+\left|\hat{N}_{r|r|}r^{2}\right|+\left|\hat{N}_{r|v|}rv\right| \\ +\left|\hat{N}_{\phi|uv|}\phi uv\right|+\left|\hat{N}_{\phi u|r|}\phi ur\right|+\left|\hat{N}_{\phi u|u|}\phi u^{2}\right|\end{array}\right) \\ &+\left[\frac{n}{100}\left(2+\frac{n}{100}\right)\left|\frac{w_{32}^{+}+w_{32}^{-}}{2}\right|+\left(1+\frac{n}{100}\right)^{2}\left(\frac{w_{32}^{+}-w_{32}^{-}}{2}\right)\right]\times\left|\hat{m}\hat{z}_{g}^{b}ur\right| \\ &+\left[\frac{n}{100}\left(2+\frac{n}{100}\right)\left|\frac{w_{33}^{+}+w_{33}^{-}}{2}\right|+\left(1+\frac{n}{100}\right)^{2}\left(\frac{w_{33}^{+}-w_{33}^{-}}{2}\right)\right]\times\left|\hat{m}\hat{x}_{g}^{b}ur\right|\end{aligned} \tag{33}$$

Further, the maximum and minimum value of g can be determined as

$$g_{\max} = \frac{1}{2}\left(-w_{31}^{-} + r_r \cdot w_{32}^{+} + LCG \cdot w_{33}^{+}\left(1+\frac{n}{100}\right)\right)\rho u_r^2 A_r \left.\frac{\partial C_{Lr}}{\partial \alpha_r}\right|_{\alpha_r=0}$$
$$g_{\min} = \frac{1}{2}\left(-w_{31}^{+} + r_r \cdot w_{32}^{-} + LCG \cdot w_{33}^{-}\left(1-\frac{n}{100}\right)\right)\rho u_r^2 A_r \left.\frac{\partial C_{Lr}}{\partial \alpha_r}\right|_{\alpha_r=0} \quad (34)$$

Finally $\hat{g}$ and γ can be determine from equations (24) and (26).

7 Controller modification

Chattering phenomenon is one of the disadvantages and important challenges in the implementation of sliding mode controllers. It is believed that there are two reasons for this phenomenon: existence of discontinues terms such as sign functions in sliding mode controller and existence of the delay in the measurement systems such as actuators. Chattering phenomenon causes high frequency oscillations around the switching variables which may damage the actuators and degrade the robustness of sliding mode controller.
Various techniques such as narrow saturation function, boundary layer method and increasing switching frequency have been proposed in the literature to reduce the effects of chattering. Integral switching variable is one of the most commonly approach which can be used to reduce the side effects of chattering and improve the system tracking capability and accuracy [23]. In this algorithm, the switching variables are rewritten according to the integration of tracking error, i.e.:

$$\sigma = \dot{\tilde{\psi}} + 2c\tilde{\psi} + c^2 \int_0^t \tilde{\psi} dt \quad (35)$$

In equation (35) we have:

$$\begin{aligned}\dot{\sigma} &= \ddot{\tilde{\psi}} + 2c\dot{\tilde{\psi}} + c^2\tilde{\psi} = \dot{r} - \ddot{\psi}_d + 2c\left(r-\psi_d\right) + c^2\tilde{\psi} \\ &= \hat{f} + \hat{g}\delta_{eq} - \ddot{\psi}_d + 2c\left(r-\psi_d\right) + c^2\tilde{\psi}\end{aligned} \quad (36)$$

The equivalent input can be redefined as follow:

$$\delta_{eq} = \frac{-\hat{f} + \ddot{\psi}_d + 2c\left(\dot{\psi}_d - r\right) - c^2\tilde{\psi}}{\hat{g}} \quad (37)$$

Finally,

$$= \frac{\hat{f} - \ddot{\psi}_d + 2c\left(r-\dot{\psi}_d\right) + c^2\tilde{\psi} + \left(\gamma F + (\gamma-1)\left|\hat{f} - \ddot{\psi}_d + 2c\left(r-\dot{\psi}_d\right) + c^2\tilde{\psi}\right| + \varepsilon\right) sign(\sigma)}{\hat{g}} \quad (38)$$

8 Simulation results

In this section, the proposed sliding mode controller based on ISV is evaluated on a naval vessel benchmark and compared with previous similar research. The benchmark is adopted from [20]. The values of the model parameters are shown in Table (1).
We assume that the reference input signal are in the sequence of 40, -10 and 20 degrees are fed in the model after a second-order critically damped system with natural frequency

$\omega_n = 0.1$ rad/s is passed through. In our evaluation, we assume that each of four parameters ship mass, gravity center, inertia and hydrodynamic coefficient are varied by 10% upwards. With this assumption, the matrices $\mathbf{W}^+$ and $\mathbf{W}^-$ are calculated using GA as follows:

$$\mathbf{W}^+ = 10^{-5}\begin{bmatrix} 0.1579 & -0.0143 & 0.0018 \\ 0.0033 & 0.0292 & 0.0000 \\ 0.0019 & -0.0001 & 0.0011 \end{bmatrix},\ \mathbf{W}^- = 10^{-5}\begin{bmatrix} 0.1196 & -0.0351 & 0.0000 \\ -0.0117 & 0.0213 & -0.0001 \\ 0.0009 & -0.0005 & 0.0009 \end{bmatrix}$$

Also the effect of waves on ship motion was simulated using 20 sinusoidal waves with different amplitudes and frequencies. These amplitudes were calculated by wave spectrum which is defined as follow:

$$\begin{aligned} S_{\zeta\zeta}(\omega) &= \frac{A}{\omega^5}\exp\left(\frac{-B}{\omega^4}\right) \\ A &= \frac{173H_{1/3}^2}{T_1^4} \\ B &= \frac{691}{T_1^4} \end{aligned} \tag{39}$$

Table 1 The ship model parameters used in simulations [20]

Symbol	Value	Symbol	Value	Symbol	Value
$\hat{Y}_{\dot{v}}$	-309300	$\hat{Y}_{\dot{r}}$	-1400000	$\hat{Y}_{\dot{p}}$	-296000
$\hat{Y}_{ur}$	131000	$\hat{Y}_{v\|v\|}$	-3700	$\hat{Y}_{v\|r\|}$	-794000
$\hat{Y}_{\phi\|uv\|}$	10800	$\hat{Y}_{\phi\|ur\|}$	251000	$\hat{Y}_{\phi uu}$	74
$\hat{K}_{\dot{v}}$	296000	$\hat{K}_{\dot{r}}$	0	$\hat{K}_{\dot{p}}$	-774000
$\hat{K}_{ur}$	-102000	$\hat{K}_{v\|v\|}$	29300	$\hat{K}_{v\|r\|}$	621000
$\hat{K}_{\phi\|uv\|}$	-8400	$\hat{K}_{\phi\|ur\|}$	-196000	$\hat{K}_{\phi uu}$	-1180
$\hat{K}_{p\|p\|}$	-416000	$\hat{K}_{p}$	500000	$\hat{K}_{\phi\phi\phi}$	$-0.325\rho g\nabla$
$\hat{N}_{\dot{v}}$	538000	$\hat{N}_{\dot{r}}$	-38700000	$\hat{N}_{\dot{p}}$	0
$\hat{N}_{\|u\|r}$	-4710000	$\hat{N}_{r\|r\|}$	-(2020)00	$\hat{N}_{r\|v\|}$	-15600000
$\hat{N}_{\phi u\|r\|}$	-4980000	$\hat{N}_{\phi u\|u\|}$	-8000	$\hat{Y}_{\|u\|v}$	-11800
ρ	1025 kg/m^3	∇	355.88 m^3	$\hat{Y}_{r\|v\|}$	-182000
r_r	2.61 m	A_p	5 m^2	LCG	20.4 m
w	0.1	t	0.1	$X_{u\|u\|}$	-1960
$\hat{K}_{\|u\|v}$	9260	$\hat{K}_{r\|v\|}$	142000	$\hat{K}_{\|u\|p}$	-15500
$\hat{N}_{\|u\|v}$	-92000	$\hat{N}_{\phi\|uv\|}$	-214000	A_r	3 m^2
$\partial C_L / \partial \alpha_r$	3.094	GMt	1 m	m	$\rho\nabla$

To simulate the condition of rough waves it is assumed that $H_{1/3} = 2.5\,m$ and $T_1 = 7.5\,s$. After producing the waves, Force Response Amplitude Operators (FRAOs) is applied to convert these waves to forces-moments using. These forces-moments are applied to the system as the environmental disturbances. Figure (2) shows tracking performance of the proposed sliding mode control method presented in (27). As can be seen from this figure, the system under study tracks the reference input with a minimum steady state error in yaw angle and very low amplitude chattering in the control signal.

The performance of the introduced sliding mode control method based on ISV is illustrated in Figure (3). As shown in this figure, the proposed control method easily tracks the input reference with zero steady-state error. Moreover, in comparison to the previous controller, the amount of chattering is reduced significantly.

As mentioned, the ship autopilot is designed in a few research works using sliding mode control method [8-11]. These controllers have a same structure based on linearized model of the system. Assuming,

$$\dot{x}_h = A_h x_h + b_h \alpha_r \qquad x_h = \begin{bmatrix} v \\ r \\ \psi \end{bmatrix}, A_h = \begin{bmatrix} a_{11} & a_{12} & 0 \\ a_{21} & a_{22} & 0 \\ 0 & 1 & 0 \end{bmatrix}, b_h = \begin{bmatrix} b_1 \\ b_2 \\ 0 \end{bmatrix} \tag{40}$$

The control input is considered as follow [12]:

$$\alpha_r = -k^T x_h - \left(h^T b_h\right)^{-1} \left[\eta_h \tanh\left(\sigma_h / \phi_h\right)\right] \tag{41}$$

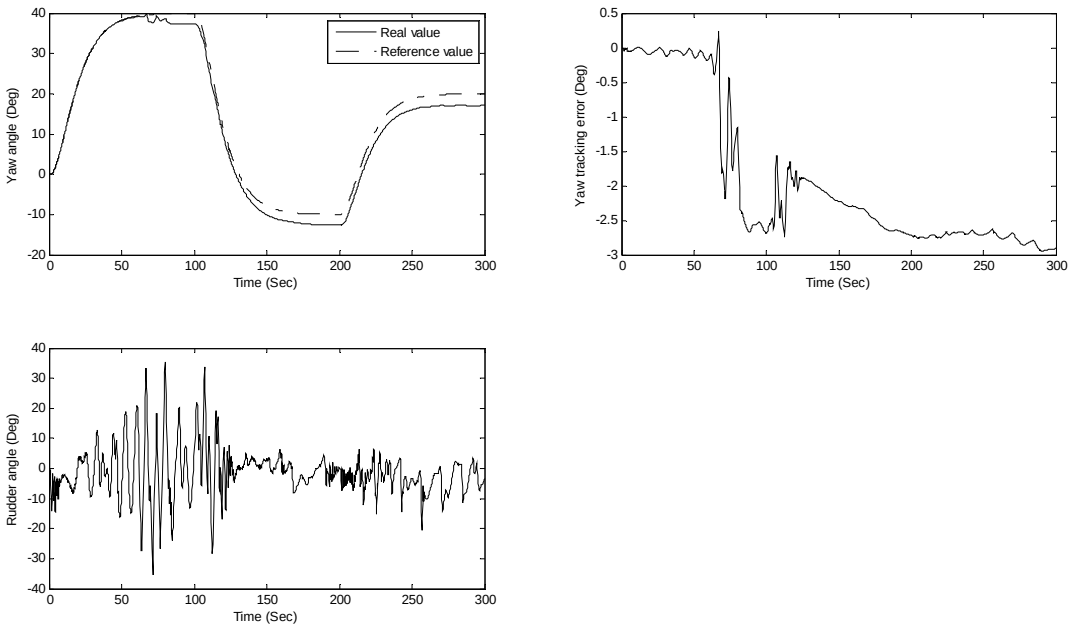

Figure 2 Input reference tracking of proposed SMC with unmodified ISV

where $\sigma_h = h_1 v + h_2 r + h_3 (\psi - \psi_d)$ is switching variable, $k = [k_1, k_2, 0]^T$ is the feedback gain, h is the right eigenvector of $A_c = A_h - b_h k^T$ and η_h is the constant gain which related to bound of uncertainty. It must be noticed that in these 3 researches, the bounds of uncertainty have not been calculated analytically. Also, the optimum values of k_1, k_2, η_h and ϕ_h have been determined by Genetic Algorithm. Figure (4) shows the simulation results of presented controller in Fang and Luo [24] based on our nonlinear model of the ship. It can be seen that the performance of the controller is nearly low.

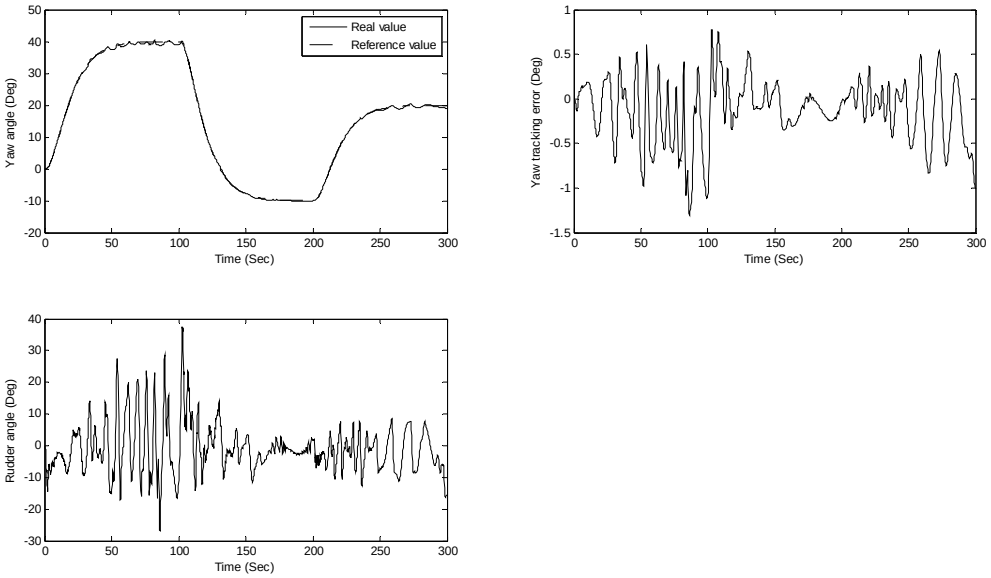

Figure 3 Input reference tracking of proposed SMC with ISV

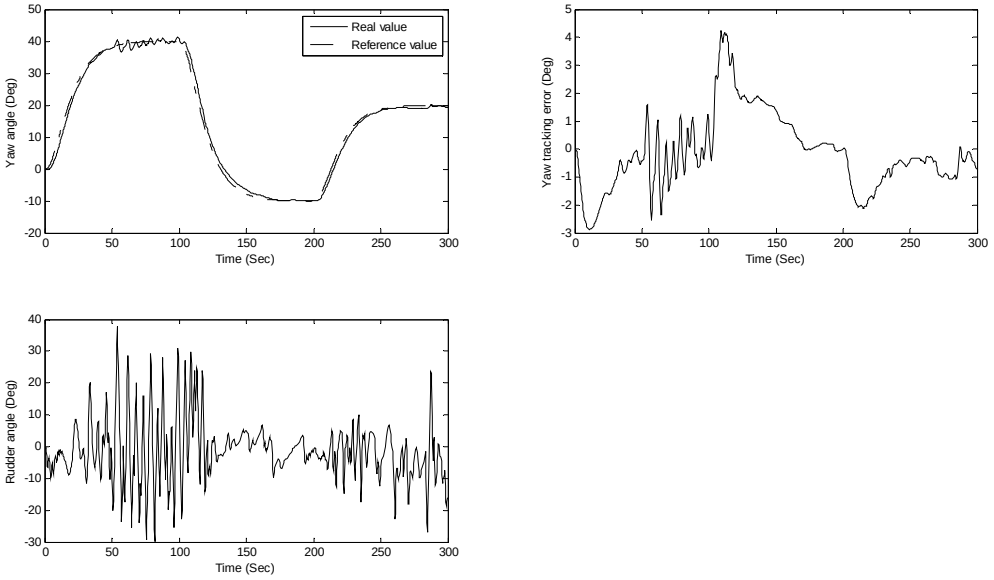

Figure 4 Simulation results of presented controller in [24]

Table 2 Performance index of the three SMC

	Primary SMC	SMC base ISV	SMC designed in [24]
Performance Index	1.92 (deg)	0.28 (deg)	1.05 (deg)

The comparative analysis of the three proposed sliding mode controllers based on performance index given in equation (42), is shown in Table (2).

$$Performance\,index = \frac{1}{t_f}\int_0^{t_f} \left|\psi - \psi_d\right| dt \tag{42}$$

As can be seen from this Table, although three controllers have almost satisfactory performance, however, the performance of the proposed SMC based on ISV is much better in terms of transient and steady state response under normal conditions and even in the presence of uncertainties.

9 Conclusion

In this paper, a sliding mode control was proposed to control an uncertain nonlinear ship autopilot system. As one of the main objectives of this study was to effectively suppress the chattering phenomenon, the modified integral switching variable was used to replace the sign function in designing the control law. Moreover, in order to improve tracking performance and to guarantee the robust stability of the nonlinear dynamic system with parameter uncertainties, model uncertainty bounds of parameters with uncertainties were determined by GA. The robustness and effectiveness of the proposed SMC based on ISV approach in terms reference tracking, disturbance rejection and model uncertainties in the presence of rough waves was confirmed by simulation results. Sliding mode controller design based on integrated control of Roll and Yaw by using fins and rudders is the future challenge.

References

[1] Wang, Y., Chai, S., and Nguyen, H.D., "Unscented Kalman Filter Trained Neural Network Control Design for Ship Autopilot with Experimental and Numerical Approaches", Applied Ocean Research, Vol. 85, pp. 162-172, (2019).

[2] Shih, C.H., Huang, P.H., Yamamura, S., and Chen, C.Y., "Design Optimal Control of Ship Maneuver Patterns for Collision Avoidance: A Review", Journal of Marine Science and Technology, Vol. 20, pp. 111-121, (2012).

[3] Jie, H., "Research on Unmanned Ship Autopilot System Based on Human Simulated Intelligent Control", Ship Science and Technology, Vol. 2017, pp. 17, (2017).

[4] Tung, L.T., "Design a Ship Autopilot using Neural Network", Journal of Ship Production and Design, Vol. 33, pp. 192-196, (2017).

[5] Liu, Z., "Ship Adaptive Course Keeping Control with Nonlinear Disturbance Observer", IEEE Access, Vol. 5, pp. 17567-17575, (2017).

[6] Ejaz, M., and Chen, M., "Sliding Mode Control Design of a Ship Steering Autopilot with Input Saturation", International Journal of Advanced Robotic Systems, Vol. 14, https://doi.org/10.1177/1729881417703568, (2017).

[7] Wang, Q., and Yang, Y., "Design of Ship Autopilot Based on Fuzzy Control Theory", Ship Science and Technology, pp. 63-71, (2018).

[8] Shen, Z., Jiang, Wang, G., and Guo, C., "Fuzzy-adaptive Iterative Sliding-mode Control for Sail-assisted Ship Motion", Journal of Harbin Engineering University, pp. 2-11, (2016).

[9] Zhang, X.K., Han, X., Guan, W., and Zhang, G.Q., "Improvement of Integrator Backstepping Control for Ships with Concise Robust Control and Nonlinear Decoration", Ocean Engineering, Vol. 189, pp. 1-7, (2019).

[10] Bhatt, A., Das, S., and Talole, S., "Robust Backstepping Ship Autopilot Design", Journal of Marine Engineering & Technology, pp. 1-8, (2018).

[11] Wang, Y., Chai, S., and Nguyen, H.D., "Experimental and Numerical Study of Autopilot using Extended Kalman Filter Trained Neural Networks for Surface Vessels", International Journal of Naval Architecture and Ocean Engineering, Vol. 12, pp. 314-324, (2020).

[12] Gupta, D., Vasudev, K., and Bhattacharyya, S., "Genetic Algorithm Optimization Based Nonlinear Ship Maneuvering Control", Applied Ocean Research, Vol. 74, pp. 142-153, (2018).

[13] Wang, S., Wang, L., Qiao, Z., and Li, F., "Optimal Robust Control of Path Following and Rudder Roll Reduction for a Container Ship in Heavy Waves", Applied Sciences, Vol. 8, pp. 1-19, (2018).

[14] Das, S., and Talole, S. E., "Robust Steering Autopilot Design for Marine Surface Vessels", IEEE Journal of Oceanic Engineering, Vol. 41, pp. 913-922, (2016).

[15] Tomera, M., "*Fuzzy Self-tuning PID Controller for a Ship Autopilot in Marine Navigation*", ed: CRC Press, pp. 93-103, Gdynia, Poland, (2017).

[16] Fossen, T.I., "*Guidance and Control of Ocean Vehicles*", Vol. 199, Wiley New York, (1994).

[17] Yuan, L., and Wu, H.s., "Terminal Sliding Mode Fuzzy Control Based on Multiple Sliding Surfaces for Nonlinear Ship Autopilot Systems", Journal of Marine Science and Application, Vol. 9, pp. 425-430, (2010).

[18] Liu, Y., Bu, R., and Gao, X., "Ship Trajectory Tracking Control System Design Based on Sliding Mode Control Algorithm", Polish Maritime Research, Vol. 25, pp. 26-34, (2018).

[19] Fossen, T.I., "A Nonlinear Unified State-space Model for Ship Maneuvering and Control in a Seaway", International Journal of Bifurcation and Chaos, Vol. 15, pp. 2717-2746, (2005).

[20] Perez, T., "*Ship Motion Control: Course Keeping and Roll Stabilisation using Rudder and Fins*", Springer Science & Business Media, Berlin, Germany, (2006).

[21] Hashimoto, H., Umeda, N., and Matsuda, A., "Importance of Several Nonlinear Factors on Broaching Prediction", Journal of Marine Science and Technology, Vol. 9, pp. 80-93, (2004).

[22] Golzari, S., Rashidi, F., and Farahani, H.F., "A Lyapunov Function Based Model Predictive Control for Three Phase Grid Connected Photovoltaic Converters", Solar Energy, Vol. 181, pp. 222-233, (2019).

[23] Harifi, A., Aghagolzadeh, A., Alizadeh, G., and Sadeghi, M., "Designing a Sliding Mode Controller for Slip Control of Antilock Brake Systems", Transportation Research Part C: Emerging Technologies, Vol. 16, pp. 731-741, (2008).

[24] Fang, M.C., and Luo, J.H., "On the Track Keeping and Roll Reduction of the Ship in Random Waves using Different Sliding Mode Controllers", Ocean Engineering, Vol. 34, pp. 479-488, (2007).